Rhodamine 123 Requires Carrier-Mediated Influx for Its Activity as a P-Glycoprotein Substrate in Caco-2 Cells

Matthew D. Troutman[1] and Dhiren R. Thakker[1,2]

Received December 6, 2002; accepted April 24, 2003

Purpose. The purpose of this work was to elucidate transport pathways of the P-glycoprotein (P-gp) substrates rhodamine 123 (R123) and doxorubicin across Caco-2 cells.

Methods. Experiments were designed to identify saturable and nonsaturable transport processes and transport barriers for R123 and doxorubicin transport across Caco-2 cells. Confocal laser scanning microscopy (CLSM) imaged R123 transport under normal conditions and in the presence of the P-gp inhibitor, GW918 (used to abolish P-gp-mediated efflux activity).

Results. R123 secretory P_{app} ($P_{app,BA}$) showed concentration dependence, whereas R123 absorptive P_{app} ($P_{app,AB}$) did not. Inhibition of P-gp efflux revealed that P-gp-mediated efflux had no effect on R123 or doxorubicin $P_{app,AB}$, but enhanced R123 and doxorubicin $P_{app,BA}$. In calcium-free medium, R123 $P_{app,AB}$ increased 15-fold, indicating intercellular junctions are a barrier to R123 absorption. CLSM of R123 fluorescence during absorptive transport under normal conditions and in the presence of GW918 was identical, and was limited to paracellular space, confirming that P-gp is not a barrier to R123 absorption. CLSM revealed that R123 fluorescence during secretory transport under normal conditions and in the presence of GW918 was localized intracellularly and in paracellular space. R123 and doxorubicin uptake across Caco-2 cells basolateral membrane was saturable.

Conclusions. R123 absorptive transport occurs primarily by paracellular route, whereas R123 secretory transport involves influx across BL membrane mediated solely by a saturable process followed by apically directed efflux via P-gp. Doxorubicin utilizes similar transport pathways to cross Caco-2 cells.

KEY WORDS: P-glycoprotein; rhodamine 123; doxorubicin; intestinal absorption; intestinal secretion.

INTRODUCTION

The multidrug efflux transporter, P-glycoprotein (P-gp), can play a significant role in the intestinal disposition of its substrates (1,2). In the intestine, P-gp is located in the apical (AP) membrane of enterocytes (3,4), where it provides a formidable barrier to the entry of foreign compounds, including drugs (5–7). In some cases, P-gp-mediated efflux activity in the intestine can reduce the oral absorption of its substrates by several-fold. Indeed, the oral absorption of drugs, like protease inhibitors, taxol, and cyclosporin A, drastically increases in the absence of P-gp-mediated efflux activity as seen in studies comparing oral absorption of these agents in P-gp-deficient mice vs. wild-type mice (8–10). In some cases, P-gp not only attenuated the oral absorption of these compounds but also facilitated hepatic and intestinal metabolism (11). Recently, evidence has also been presented demonstrating that P-gp-mediated efflux activity acts to make intestinal exsorption an important route of elimination for some P-gp substrates (10,12–14). The substrate specificity of P-gp is broad, P-gp-mediated efflux activity is saturable, and P-gp expression in the intestine can be variable. Consequently, the potential for nonlinear oral absorption and for drug–drug interactions involving P-gp substrates, inhibitors, and/or inducers certainly exists and has been well documented (1,15). These important therapeutic concerns make the study of P-gp-mediated efflux activity in models of polarized epithelium (especially the intestine) critical. A commonly used method to gauge the functional activity of P-gp in these models involves measuring the transport of a known P-gp substrate in the absorptive and secretory transport direction, and then calculating an efflux ratio (secretory Papp/absorptive Papp). Large efflux ratios for the control substrate are assumed to be due to high P-gp-mediated efflux activity in the model.

The cationic hydrophilic P-gp substrate, rhodamine 123 (R123; Ref. 16; Fig. 1), has been used extensively as a probe substrate to assess the functional activity of P-gp in a variety of cell lines and assays, including the National Cancer Institute (NCI) screen for the presence of P-gp (17). In the NCI screen, compounds that inhibit R123 efflux from preloaded P-gp-expressing cells are determined to be P-gp substrates or inhibitors. Several assays in the intestinal epithelium and Caco-2 cell monolayers have used altered R123 transport as a marker to quantify changes in P-gp-mediated efflux activity in response to a wide variety of treatments (18–22). In many of these studies, a decrease in the efflux ratio of R123 was assumed to be due to inhibition of P-gp-mediated efflux activity by the treatment (18–21). Despite the widely accepted use of R123 transport as a marker for P-gp-mediated efflux activity in intestinal epithelium and Caco-2 cell monolayers, the mechanism of R123 transport across intestinal epithelium and Caco-2 cells in the absorptive and secretory directions is unknown. It is often assumed that R123 absorptive and secretory transport occurs by similar processes, namely via transcellular passive diffusion. Recent reports have shown that R123 transport in renal cells involves mechanisms other than passive diffusion and P-gp-mediated efflux. For example, in addition to P-gp, R123 can be transported by the organic cation transport system in renal cells (23–25).

In the present study, we have elucidated the mechanism of R123 transport across Caco-2 cell monolayers, a model for intestinal epithelium. Our studies show that indeed the mechanisms underlying absorptive and secretory transport of R123 across Caco-2 cell monolayers are completely different, such that P-gp plays no role in altering its absorptive transport but significantly enhances the secretory transport. Finally, we show that P-gp has a similar asymmetric effect on the absorptive and secretory transport across Caco-2 cells of the important anticancer drug doxorubicin (Fig. 1).

MATERIALS AND METHODS

Materials

The Caco-2 cell line, Caco-2 cell clone P27.7 (26), was obtained from Mary F. Paine, PhD and Paul B. Watkins, MD

[1] Division of Drug Delivery and Disposition, School of Pharmacy, the University of North Carolina at Chapel Hill, Chapel Hill, Chapel Hill, North Carolina 27599.

[2] To whom correspondence should be addressed. (dhiren_thakker@unc.edu)

0724-8741/03/0800-1192/0 © 2003 Plenum Publishing Corporation

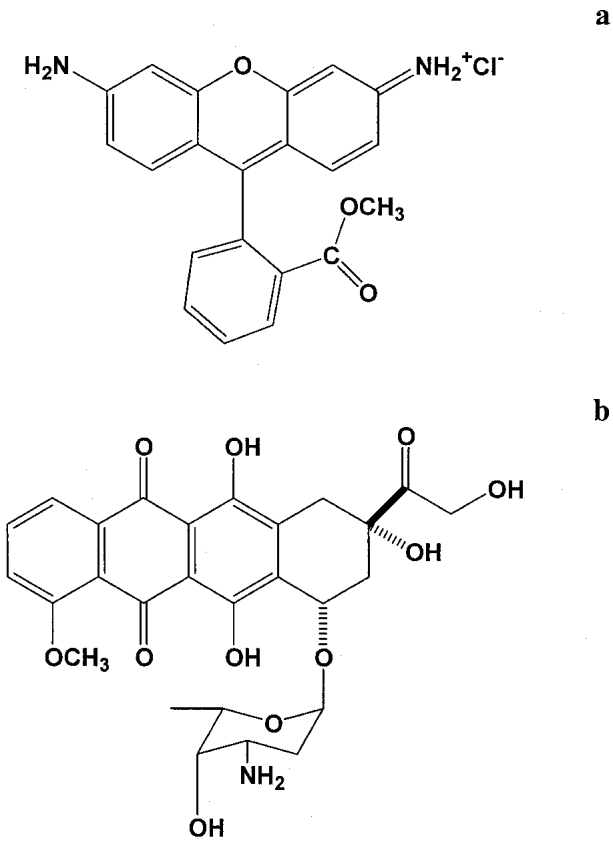

Fig. 1. Structures of the hydrophilic cationic substrates, rhodamine 123 (a) and doxorubicin (b). Calculated pK_a for rhodamine 123 and doxorubicin are 6.12 ± 0.40 (amine) and 9.67 ± 0.70 (amine), respectively. Rhodamine 123 and doxorubicin log D values have been determined (at pH 7.4) to be 0.53 (34) and 0.38 (36), respectively.

(the University of North Carolina at Chapel Hill, Chapel Hill, NC, USA). Eagle's minimum essential medium with Earle's salts and L-glutamate, fetal bovine serum, nonessential amino acids (×1000), 0.05% trypsin–EDTA solution, and penicillin–streptomycin–amphotericin B solution (×1000) were obtained from Gibco Laboratories (Grand Island, NY, USA) or from Sigma Chemical Co. (St. Louis, MO, USA). Hank's balanced salt solution was obtained from Mediatech Inc. (Herndon, VA, USA). *N*-hydroxyethylpiperazine-*N*′-2-ethanesulfonate (1 M), was obtained from Lineberger Comprehensive Cancer Center, the University of North Carolina at Chapel Hill (Chapel Hill, NC, USA). D-(+)-glucose, doxorubicin, Triton X-100, and R123 were purchased from Sigma Chemical Co. The bicinchoninic acid assay kit for total protein determination was obtained from Pierce Chemical Company (Rockford, IL, USA). Transwells™ were obtained from Corning Costar (Cambridge, MA, USA). GW918 was provided by Kenneth Brouwer, PhD (GlaxoSmithKline, Research Triangle Park, NC, USA).

Cell Culture

Caco-2 cells were cultured as described previously (27,28). Briefly, cells were cultured at 37°C in minimum essential medium, supplemented with 10% fetal bovine serum, 1% nonessential amino acids, 100 U/mL penicillin, 100 μg/mL streptomycin, and 0.25 μg/mL amphotericin B in an atmosphere of 5% CO_2 and 90% relative humidity. The cells were passaged (cells were isolated using trypsin–EDTA) upon reaching approximately 80–90% confluency and plated at densities of 1:5, 1:10, or 1:20 in T-flasks. Caco-2 cells (passage number 47 to 57) were seeded at a density of 60,000 cells/cm^2 on polycarbonate membranes of Transwells™ (12 mm id, 3.0-μm pore size). Medium was changed the day after seeding, and every other day thereafter. Medium was added to apical (AP) and basolateral (BL) compartments. The cell monolayers were used approximately 21 days post-seeding.

Transport Experiments

Cell monolayers were incubated in transport buffer (TBS: Hanks balanced salt solution with 25 mM D-glucose and 10 mM *N*-hydroxyethylpiperazine-*N*′-2-ethanesulfonate, pH 7.4) with 1% (v/v) dimethylsulfoxide (DMSO) for 30 min at 37°C (temperature maintained throughout the experiment). To check cell monolayer integrity, the transepithelial electrical resistance (TEER) was measured using an EVOM Epithelial Tissue Voltammeter and an Endohm-12 electrode (World Precision Instruments, Sarasota, FL, USA). Caco-2 cells with TEER values ≥ 300 Ω·cm^2 were used in the transport experiments. Donor solutions of test compound with 1% (v/v) DMSO in TBS were added to the donor compartment—for absorptive (AP to BL) transport, donor is AP compartment, and for secretory (BL to AP) transport, donor is BL compartment. Test compound flux was measured in both transport directions following the lag phase (period where flux was not linear with time because of binding of compound) when flux is linearly related to time, and under sink conditions (less than 10% of the initial concentration in the donor compartment appearing in the acceptor side per given time interval). At the completion of all experiments, TEER was measured to ensure that cell monolayer integrity and viability had not been adversely affected by the experimental conditions. To determine the transport in the absence of P-gp-mediated efflux activity, flux was measured as described above in the presence of GW918 (1 μM; a concentration approx. 30-fold greater than the reported K_i of 35 nM; Ref. 29) added to donor and acceptor solutions.

To determine the relative contribution of transcellular vs. paracellular transport of R123, the flux of R123 was measured as described above and under conditions that allowed free access to the paracellular space by disrupting the tight junctions (Ca^{2+}/Mg^{2+}-free incubation medium; Ref. 28).

Confocal Laser Scanning Microscopy (CLSM) Experiments

Caco-2 cells were incubated with R123 or R123 plus GW918 (1.0 μM), in TBS with 1% (v/v) DMSO (R123 placed in the appropriate donor compartment) for 20 min. The cells were then washed five times with TBS and subsequently maintained in TBS. The polycarbonate membrane was excised from the Transwell™ insert using a scalpel and mounted on a glass slide with a cover slip. Images were captured using a Zeiss confocal microscope (Carl Zeiss Inc., Gottingen, Germany) with a 63× objective and a zoom factor of 40. The image was taken approximately 10 μm above the interface of the polycarbonate membrane and the basolateral membrane.

Uptake Experiments

Cell monolayers were incubated in TBS with 1% DMSO and GW918 (1.0 μM), pH 7.4, for 30 min at 37°C (temperature maintained throughout the experiment). Donor solutions of test compound with 1% DMSO and GW918 (1.0 μM) in TBS were added to the BL compartment, and TBS with GW918 (1.0 μM) was added to AP compartment. After incubation for predetermined times (the linear phase of uptake was between 5 and 10 min for R123, and 5 and 25 min for doxorubicin, for each concentration) polycarbonate membranes of Transwell™ inserts were excised with a scalpel and dissolved in 1% Triton X-100 solution for at least 4 h before analysis (three monolayers per time point and concentration).

Sample Analysis

R123 samples were analyzed by measuring fluorescence with a LS 50B Luminescence Spectrometer (Perkin Elmer, Norwalk, CT, USA) set to excitation wavelength of 500 nm and emission wavelength of 525 nm. Doxorubicin samples were analyzed by high-performance liquid chromatography (Hewlett Packard, 1100 series, Wald Bronn, Germany) with a 100 × 3 mm C18 Aquasil column (5 μM; Keystone Scientific, Inc. Bellefonte, PA, USA), eluted with an isocratic mobile phase consisting of 65% 25 mM phosphate buffer, pH 3.5, and 35% acetonitrile at a flow rate of 1 mL/min, detection at 480 nm (using UV-Vis detection). Retention time of doxorubicin was 1.8 min.

Data Analysis

Transport Experiments

Flux was calculated using Eq. (1):

$$J = \frac{1}{A} \cdot \frac{dQ}{dt} \tag{1}$$

where A is the surface area of the porous membrane in cm^2 and Q is the amount of compound transported over time t of the experiment. Eq. (2) was used to determine the P_{app} from the flux:

$$P_{app} = \frac{J}{C_D} \tag{2}$$

where C_D is the initial concentration of the test compound added to the donor compartment.

Uptake Experiments

The uptake flux (J_{Uptake}) of R123 and doxorubicin across the BL membrane of Caco-2 cell monolayers was determined using Eq. (3):

$$J_{Uptake} = \frac{dQ}{dt} \cdot \frac{1}{\text{mg} \cdot \text{protein}} \tag{3}$$

where Q is the amount of compound taken up by the Caco-2 cell monolayer at time points 1 and 2 (for R123, time points are 5 and 10 min, and for doxorubicin, time points are 5 and 25 min), normalized to mg protein (determined by bicinchoninic acid assay to be 0.48 mg/cm^2). Data were analyzed using WinNonlin nonlinear least-squares regression analysis software (PharSight Corporation, Mountain View, CA, USA). Parameter estimates obtained from nonlinear regression analysis were reported ± standard error.

pK_a Calculation

Calculated pK_a values were generated for R123 and doxorubicin using ACD labs pK_a database software (Advanced Chemistry Development, Toronto, Canada).

RESULTS

Absorptive and Secretory Transport of R123 across Caco-2 Cell Monolayers

Over a wide concentration range (5 to 1000 μM) of R123, secretory P_{app} ($P_{app,BA}$) values were >10-fold higher than the corresponding absorptive P_{app} ($P_{app,AB}$) values (Fig. 2), indicating that R123 transport across Caco-2 cell monolayers was apically polarized. This is consistent with the presence and activity of P-gp in the AP membranes of Caco-2 cells (30,31). Interestingly, $P_{app,AB}$ remained nearly constant (approx. 1.5 × 10^{-6} cm/s) over the entire concentration range. This was surprising because P-gp-mediated efflux of R123 is a saturable process, and it was expected that as concentration was increased above certain value the attenuation of absorptive transport mediated by P-gp would decrease, resulting in progressive increases in $P_{app,AB}$. Even at concentrations up to 74-fold greater than the reported K_m (13.5 μM; Ref. 32) for P-gp mediated efflux of R123, $P_{app,AB}$ of R123 did not increase. $P_{app,BA}$ remained unchanged from 5 to 100 μM (approx. 1.6 × 10^{-6} cm/s) and then progressively decreased as concentration increased from 100 μM to 1000 μM, presumably because of saturation of P-gp. It is noteworthy that $P_{app,BA}$ remained significantly greater than $P_{app,AB}$, even at 1000 μM R123.

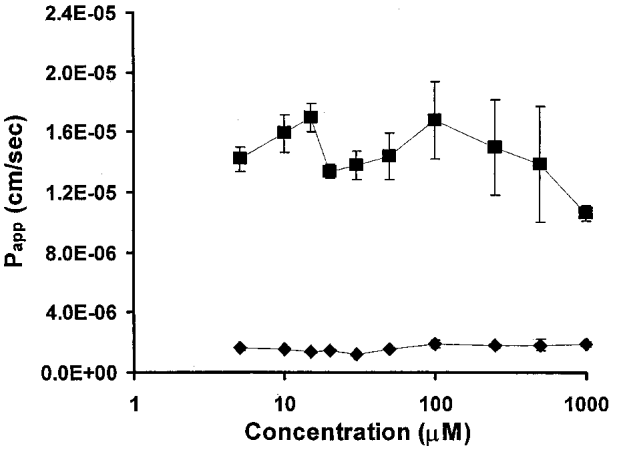

Fig. 2. Concentration dependence of rhodamine 123 P_{app} in absorptive and secretory directions across Caco-2 cell monolayers. Rhodamine 123 P_{app} at each concentration for each transport direction was measured in triplicate. Absorptive transport (♦), secretory transport (■). Data are shown as mean ± SD.

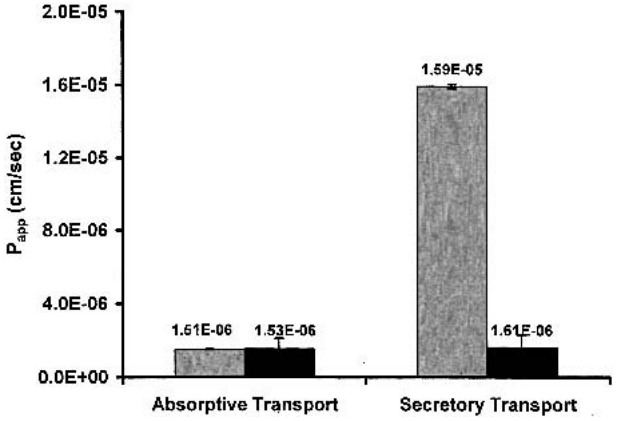

Fig. 3. Effects of the P-gp Inhibitor GW918 (1μM) on the absorptive and secretory transport of rhodamine 123 across Caco-2 cell monolayers. Transport under normal conditions: gray bars. Transport in the presence of GW918: black bars. Rhodamine 123 transport under each condition for each transport direction was measured in triplicate. Addition of GW918 (1 μM) completely abolished P-gp-mediated efflux activity. Data are shown as mean ± SD.

R123 Transport in the Presence of the P-gp Inhibitor, GW918

Figure 3 depicts $P_{app,AB}$ and $P_{app,BA}$ of R123 (10 μM), determined in the presence of the P-gp inhibitor GW918 (1 μM) and under normal conditions. In the presence of GW918, the apically directed polarity in R123 transport ($P_{app,BA}/P_{app,AB} > 10$) was completely abolished ($P_{app,AB} = P_{app,BA}$). Thus, the apically directed transport polarity of R123 across Caco-2 cells, observed under normal conditions, was completely mediated by P-gp efflux activity. Interestingly, $P_{app,AB}$ of R123, determined in the presence of GW918 was nearly equal to that determined under normal conditions. This result revealed the surprising finding that P-gp-mediated efflux activity was not a barrier to R123 absorptive transport across Caco-2 cell monolayers, and that the apically directed transport polarity of R123 across Caco-2 cell monolayers was solely due to a 10-fold enhancement of $P_{app,BA}$ of R123 conferred entirely by P-gp-mediated efflux activity.

Transcellular vs. Paracellular Transport of R123

The results depicted in Figs. 2 and 3 suggested that the absorptive transport of R123 was not affected by P-gp. Furthermore, $P_{app,AB}$ for R123 was quite low, typical of the P_{app} value of a paracellular marker, such as fluorescein (Table I; Ref. 33). Thus it is conceivable that R123 crossed the Caco-2 cell monolayers in the absorptive direction primarily via the paracellular route. This was consistent with a partial positive charge (calculated pK_a 6.1) and low log D (log D = 0.53; Ref. 34) of R123 at pH 7.4 (Fig. 1). This hypothesis was tested by measuring absorptive and secretory transport of R123 under normal conditions or in Ca^{2+}/Mg^{2+}-free transport medium (Table I). The integrity of the intercellular tight junctions is compromised in the absence of extracellular Ca^{2+}/Mg^{2+}, and thus the transmonolayer flux of a paracellularly transported compound increases significantly under this experimental condition (28). This was evidenced by the 28-fold increase in the $P_{app,AB}$ of a marker for paracellular transport, fluorescein, in the absence of Ca^{2+}/Mg^{2+} (Table I). The $P_{app,AB}$ of R123 increased by 16-fold in the absence of Ca^{2+}/Mg^{2+}, confirming our hypothesis that the absorptive transport of R123 across Caco-2 cell monolayers occurs predominantly via the paracellular route. In contrast, $P_{app,BA}$ of R123 increased by less than 2-fold in the absence of Ca^{2+}/Mg^{2+}, suggesting that transport in this direction was predominantly transcellular. As shown in Table I, the $P_{app,AB}$ of a marker for transcellular transport, theophylline (35), was only marginally increased when the transport medium was depleted of Ca^{2+}/Mg^{2+}.

Cellular Disposition of R123 during Absorptive and Secretory Transport across Caco-2 Cell Monolayers: CLSM Imaging

Caco-2 cells were imaged using CLSM to determine the cellular disposition of R123 during its absorptive and secretory transport in the presence and absence of GW918 (1 μM; Fig. 4). During absorptive transport, R123 fluorescence was limited to the paracellular space (Fig. 4A). In contrast, R123 fluorescence during secretory transport was localized intracellularly as well as in the paracellular space (Fig. 4B). Even during absorptive transport in the presence of GW918, R123 fluorescence remained localized to the paracellular space (Fig. 4C). These results provided visual evidence, confirming the results reported in Fig. 3, that P-gp does not pose a barrier to the absorptive transport of R123 across Caco-2 cell monolayers. More specifically, these results clearly showed that R123 did not cross the AP membrane of Caco-2 cell monolayers.

Comparison of Fig. 4B and D, depicting CLSM images of R123 during its secretory transport under normal conditions and in the presence of GW918, respectively, showed that R123 intracellular fluorescence was increased somewhat when P-gp-mediated efflux activity was completely inhibited during secretory transport. This was likely the result of a

Table I. R123, Fluorescein, and Theophylline Transport under Normal and Ca^{2+}/Mg^{2+}-Free Transport Buffer (TBS) across Caco-2 Cell Monolayers

Substrate (transport direction)	P_{app} (cm/s) × 10^6		Fold difference
	Normal TBS	Ca^{2+}/Mg^{2+}-free TBS	(P_{app} Ca^{2+}, Mg^{2+}-free TBS/ P_{app} normal TBS)
R123 10 μM (absorptive)	1.42 ± 0.180	22.5 ± 3.70	16
R123 10 μM (secretory)	16.2 ± 1.52	26.1 ± 3.00	1.6
Fluorescein 50 μM (absorptive)	0.810 ± 0.091	22.8 ± 2.67	28
Theophylline 50 μM (absorptive)	79.9 ± 2.97	97.1 ± 3.03	1.2

Note: Transport of each substrate under each condition was measured in triplicate. Data are shown as mean ± SD.

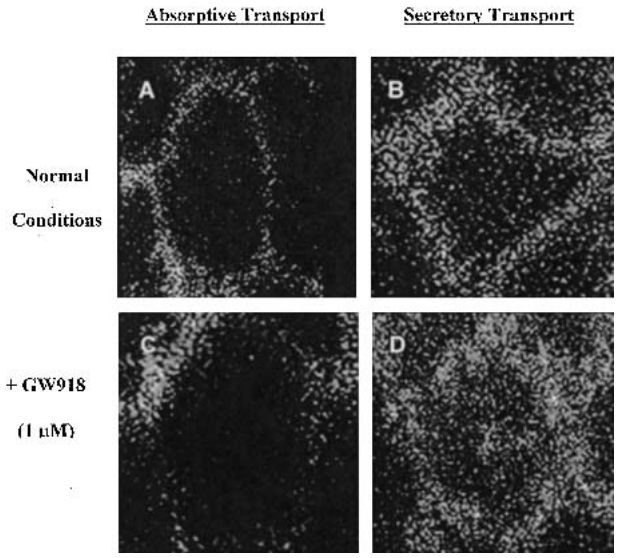

Fig. 4. Cellular disposition of rhodamine 123 during absorptive and secretory transport across Caco-2 cell monolayers. Confocal laser scanning microscopic images of rhodamine 123 (10 μM) transport across Caco-2 cell monolayers were captured using a 63× objective and a zoom factor of 40. Images were taken approximately 10 μm above the interface of the polycarbonate membrane and basolateral membrane. A and B, transport under normal conditions. C and D, transport in the presence of GW819 (1 μM). A and C, absorptive transport. B and D, secretory transport.

greater amount of R123 trapped in the cell when P-gp-mediated efflux was blocked.

R123 Uptake across the BL Membrane of Caco-2 Cell Monolayers

The concentration dependence of R123 uptake across the BL membrane in the presence of GW918 was measured to determine if R123 crossed the BL membrane via a saturable (i.e., carrier-mediated) or a nonsaturable (possibly passive diffusion) process (Fig. 5). Kinetic analysis showed that R123 uptake across the BL membrane was a saturable process, best described by a multiple binding site model. Parameters estimates obtained from nonlinear regression analysis were as follows: K_m = 173 ± 26.3 μM, γ = 1.79 ± 0.346, and J_{max} = 988 ± 85.9 pmol/min/mg protein. These data suggested that uptake of R123 across BL membrane occurred by a saturable process.

The Role of P-gp-Mediated Efflux Activity in the Absorptive and Secretory Transport of Doxorubicin across Caco-2 Cell Monolayers

The lack of P-gp effect on the absorptive transport of the model P-gp substrate, R123, raised an important question: are there therapeutic agents with similar physicochemical properties (i.e., hydrophilic organic cations) for which the absorptive transport is unaffected by P-gp-mediated efflux activity, despite large ratios of $P_{app,BA}$ to $P_{app,AB}$ values (efflux ratios)? Hence, the absorptive and secretory transport of the hydrophilic (log D = 0.38; Ref. 36) organic cation, doxorubicin (Fig. 1), across Caco-2 cell monolayers was assessed under normal conditions, and in the presence of the P-gp inhibitor GW918 (Fig. 6). As seen for R123 (Fig. 3), $P_{app,AB}$

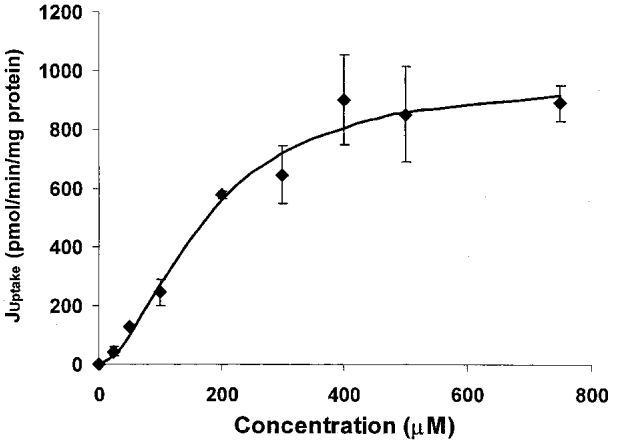

Fig. 5. Rhodamine 123 Uptake flux (J_{Uptake}) across the BL membrane of Caco-2 cell monolayers in the presence of GW918 (1 μM) as a function of concentration. Solid line represents J_{Uptake} fitted to a multiple binding site saturable kinetic model with the following parameters: K_m = 173 ± 26.3 μM, γ = 1.79 ± 0.346, and J_{max} = 988 ± 85.9 pmol/min/mg protein. Experiments were conducted in the presence of GW918 (1 μM), which completely inhibited P-gp-mediated efflux activity. Parameters estimates are reported ± standard error.

of doxorubicin (10 μM) across Caco-2 cells was nearly identical in the presence of GW918 vs. normal conditions, indicating P-gp was not a barrier to the absorptive transport of doxorubicin. The apically directed transport polarity observed for doxorubicin in the presence of P-gp-mediated efflux activity was almost entirely caused by the 40-fold enhancement in $P_{app,BA}$ of doxorubicin mediated entirely by P-gp efflux activity.

Uptake of Doxorubicin across the BL Membrane of Caco-2 Cell Monolayers

The concentration-dependence of doxorubicin uptake was quantified in order to elucidate the mechanisms by which the drug crosses the BL membrane of Caco-2 cells. Doxoru-

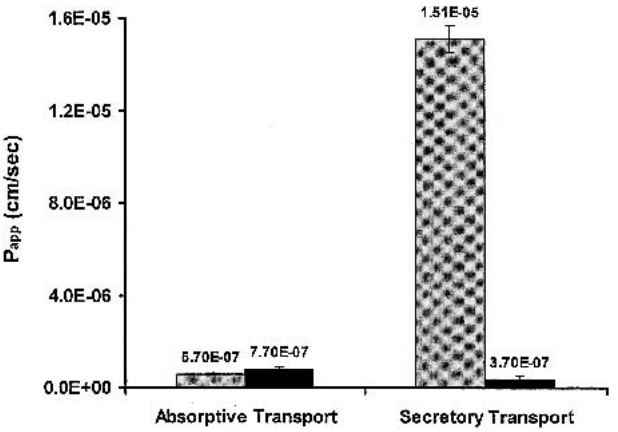

Fig. 6. Effect of the P-gp Inhibitor GW918 (1μM) on the absorptive and secretory transport of doxorubicin across Caco-2 cell monolayers. Transport under normal conditions: gray bars. Transport in the presence of GW918: black bars. Doxorubicin transport in each direction and in each condition was measured in triplicate. Addition of GW918 (1 μM) completely abolished P-gp-mediated efflux activity. Data are shown as mean ± SD.

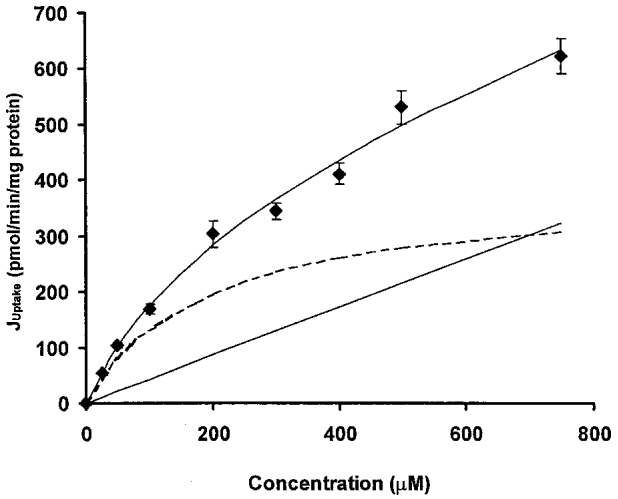

Fig. 7. Doxorubicin uptake flux (J_{Uptake}) across the BL membrane of Caco-2 cell monolayers in the presence of GW918 (1 μM) as a function of concentration. Doxorubicin J_{Uptake} across BL membrane is mediated by a combination of saturable and nonsaturable processes. The broken line represents saturable J_{Uptake} fitted to the following parameters: K_m = 198 ± 73.5 μM and J_{max} = 417 ± 159 pmol/min/mg protein. The stippled line represents nonsaturable J_{Uptake} fitted to the following parameter: K_d = 0.462 ± 0.173 ml/min/mg protein. The solid line represents total J_{Uptake} fitted using the parameters determined for nonsaturable and saturable processes. Experiments were conducted in the presence of GW918 (1 μM), which completely abolished P-gp-mediated efflux activity. Parameters estimates are reported ± standard error.

bicin uptake across the BL membrane involved a combination of saturable and nonsaturable processes (Fig. 7). The uptake process was described by a K_m of 198.3 μM and J_{max} of 417.3 pmol/min/mg protein for the saturable component, and by a K_d of 0.462 mL/min/mg protein for the nonsaturable component.

DISCUSSION

R123 (Fig. 1), a P-gp substrate (16), has been extensively used as a marker for P-gp-mediated efflux activity in polarized intestinal epithelium (18–22). Typically, the polarity observed in the transport of this probe substrate, i.e., greater secretory flux than absorptive flux, is used as evidence for P-gp-mediated efflux activity in the intestinal epithelium, or *in vitro* cell culture models of intestinal epithelium, such as Caco-2 cell monolayers. Alterations in the ratio of secretory to absorptive permeability of R123 across polarized epithelium have been used to characterize how treatments affect intestinal P-gp-mediated efflux activity. It is assumed that other than P-gp-mediated efflux across the AP membrane, the absorptive and secretory transport of R123 occurs via a transcellular passive diffusion process. It is also assumed that the polarity in the bidirectional transport experiments using R123 as a probe substrate is caused by the attenuation of its absorptive transport and enhancement of secretory transport conferred by P-gp-mediated efflux activity.

Our results elucidate the absorptive and secretory transport pathways for R123 across Caco-2 cell monolayers, an *in vitro* cell culture model of the intestinal epithelium that expresses functionally active P-gp in the AP membrane (31). These findings lead to important conclusions regarding: 1) the role P-gp plays in altering the absorptive and secretory transport of cationic hydrophilic P-gp substrates such as R123 and doxorubicin (Fig. 1); 2) the transport pathways these cationic hydrophilic compounds exploit to cross polarized epithelium; and 3) the implications of using R123 (and doxorubicin) as probes for P-gp-mediated efflux activity in polarized epithelium.

As expected, R123 transport was apically polarized under normal conditions. Under conditions that abolished P-gp-mediated efflux activity (in the presence of GW918), R123 $P_{app,AB}$ was nearly identical to R123 $P_{app,BA}$. This result clearly confirmed that P-gp-mediated efflux activity is entirely responsible for conferring apically directed polarity to R123 transport. Unexpectedly, R123 absorptive transport was not affected by P-gp-mediated efflux activity although it is a P-gp substrate; thus, the polarity conferred by P-gp to R123 transport was entirely due to enhancement of the secretory transport. The $P_{app,AB}$ of R123 was low, similar in magnitude to that of the paracellular marker fluorescein, and concentration-independent (Figs. 2 and 3, Table I). Furthermore, intercellular junctions highly restricted R123 absorptive transport in the presence or absence of P-gp-mediated efflux activity—a characteristic of molecules that cross the monolayer via the paracellular pathway (28). These results suggest that the absorptive transmonolayer translocation of R123 occurs predominately by a passive diffusion process via the paracellular pathway. The reason R123 utilizes this pathway during absorption is not because transcellular transport is attenuated by P-gp-mediated efflux activity (Fig. 8). Under normal conditions, or in conditions that completely inhibited P-gp-mediated efflux activity (in the presence of GW918), R123 fluorescence observed (using CLSM) during its absorptive transport was limited to the paracellular space. Taken together, these results lead to a very important finding: when present on the AP side of the Caco-2 cell monolayer, R123 does not cross the cell membrane and consequently enter the cells. The entry of R123 into the cells is not prevented by P-gp-mediated efflux; rather it is caused by the inability of R123 to cross the lipid bilayer, consistent with its low log D

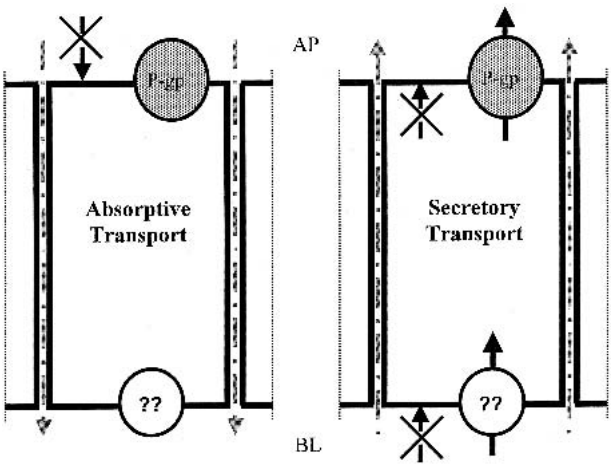

Fig. 8. Proposed rhodamine 123 transport pathways across Caco-2 cell monolayers. Dashed black lines represent passive transcellular flux; dashed gray lines represent paracellular flux; solid black lines represent carrier-mediated flux.

value and partial positive charge (see Fig. 1). Indeed, it has been shown that R123 can only bind to P-gp after entering the cytosol, indicating that the binding site of P-gp for R123 is located either within the cytosol, or within the cytosolic-inner leaflet interface (37). Therefore, P-gp cannot affect R123 absorptive transport because this molecule does not enter the cytosol (to access this binding site) during absorptive transport.

The secretory transport of R123 across Caco-2 cells in the presence of P-gp-mediated efflux activity occurs by a completely different pathway than the absorptive transport (Fig. 8). Our results show that during its secretory transport, R123 uses the transcellular pathway (Fig. 4) by first crossing the BL membrane via a saturable mechanism (Fig. 5), and then crossing the AP membrane via P-gp-mediated efflux (Fig. 3). The transcellular transport of R123 in the secretory direction occurs completely by saturable processes (Fig. 5). It is important to note that the BL membrane of Caco-2 cells is nearly identical to that of unpolarized cells with respect to plasma membrane composition (38). Our finding that R123 uptake across the BL membrane occurs entirely via a saturable process suggests that R123 does not passively diffuse across unpolarized (like the BL membrane of Caco-2 cells) or polarized (like the AP membrane of Caco-2 cells) cell membranes, and entry into the cell must be mediated by an uptake transporter. These findings are consistent with the reports that cellular uptake of R123 in MV522 and MV522/Q6 cells (23), is carrier mediated. In the secretory direction, R123 transport from cytosol across AP membrane is mediated by P-gp efflux activity. In the absence of P-gp-mediated efflux activity, R123 taken up into the cell via carrier-mediated uptake across the BL membrane does not cross the AP membrane, and is trapped inside the cells. This was evident from the very low $P_{app,BA}$ of R123 when P-gp was inhibited by GW918 (Fig. 3), despite significant uptake of R123 (Figs. 4 and 5) under these experimental conditions.

Our studies show that compounds with physicochemical properties like those of R123, i.e., hydrophilic organic cations, may be substrates for P-gp, and yet their absorption across intestinal epithelium will not be attenuated by P-gp-mediated efflux activity. The large apically directed transport polarity observed for these compounds may lead one to the false conclusion that P-gp is responsible for their limited absorption. Large apically directed transport polarity observed for hydrophilic organic cations may be the result of two major reasons. First, the inability of these hydrophilic organic cations to cross the AP membrane necessitates that absorptive transport occur nearly entirely via the paracellular pathway. Transport via the paracellular pathway is typically inefficient (compared to transport via the transcellular pathway), and results in low P_{app} values (28). Second, the uptake of these compounds across the BL membrane can occur efficiently via an apically directed uptake transporter localized to the BL membrane, followed by efflux from the intracellular space across the AP membrane via P-gp. We have shown that the chemotherapeutic agent doxorubicin, with a basic pK_a of 9.7 and low log D value of 0.38 (see Fig. 1; Ref. 36) behaves very similarly to R123 with respect to its absorptive and secretory transport mechanisms across Caco-2 cell monolayers, and with respect to the role P-gp-mediated efflux activity plays in affecting its absorptive and secretory transport processes (Figs. 5 and 6). Examples of other cationic hydrophilic P-gp substrates that show similar transport behavior include tetramethylrosamine chloride (unpublished data), cimetidine and ranitidine (39). Additionally, we have observed qualitatively identical results with regards to how P-gp affects the transport (both directions) of R123 and doxorubicin in MDCK and MDR-MDCK cell monolayers (40).

Finally, these findings have important consequences for the use of R123 as a test substrate for P-gp-mediated efflux activity in any cell system. R123 can only be used as a probe for P-gp-mediated efflux activity when: 1) a transporter-mediated uptake system for R123 is present and is not rate limiting to P-gp-mediated efflux activity, and 2) experimental conditions do not affect the transporter mediating R123 uptake. Based on studies performed in LLC-PK1 and LLC-PK1:MDR cells, it has been suggested that the use of doxorubicin as a marker for P-gp-mediated efflux activity would be preferred to R123 because R123 is subject to additional apically directed transport via the organic cation transport system in these cells, whereas doxorubicin is not (25). Based on the results of our studies following doxorubicin transport across Caco-2 cells, we conclude that caution must also be exercised before doxorubicin is chosen as the marker for P-gp-mediated efflux activity.

ACKNOWLEDGMENTS

Financial support for this research was provided by a fellowship from the PhRMA Foundation and by grants from DuPont Pharmaceuticals Company and Parke-Davis. GW918 was kindly provided by Dr. Ken Brouwer and GlaxoSmith-Kline, RTP, NC. The Caco-2 cell line was kindly provided by Drs. Mary F. Paine and Paul Watkins of the University of North Carolina at Chapel Hill, Chapel Hill, NC.

REFERENCES

1. M. F. Fromm. P-glycoprotein: a defense mechanism limiting oral bioavailability and CNS accumulation of drugs. *Int. J. Clin. Pharmacol. Ther.* **38**:69–74 (2000).
2. J. A. Silverman. Multidrug-resistance transporters. *Pharm. Biotechnol.* **12**:353–386 (1999).
3. S. Hsing, Z. Gatmaitan, and I. M. Arias. The function of Gp170, the multidrug-resistance gene product, in the brush border of rat intestinal mucosa. *Gastroenterology* **102**:879–885 (1992).
4. F. Thiebaut, T. Tsuruo, H. Hamada, M. M. Gottesman, I. Pastan, and M. C. Willingham. Cellular localization of the multidrug-resistance gene product P- glycoprotein in normal human tissues. *Proc. Natl. Acad. Sci. USA* **84**:7735–7738 (1987).
5. P. Borst, A. H. Schinkel, J. J. Smit, E. Wagenaar, L. Van Deemter, A. J. Smith, E. W. Eijdems, F. Baas, and G. J. Zaman. Classical and novel forms of multidrug resistance and the physiological functions of P-glycoproteins in mammals. *Pharmacol. Ther.* **60**:289–299 (1993).
6. P. Borst and A. H. Schinkel. What have we learnt thus far from mice with disrupted P-glycoprotein genes? *Eur. J. Cancer* **32A**: 985–990 (1996).
7. B. L. Lum and M. P. Gosland. MDR expression in normal tissues. Pharmacologic implications for the clinical use of P-glycoprotein inhibitors. *Hematol. Oncol. Clin. North Am.* **9**:319–336 (1995).
8. R. B. Kim, M. F. Fromm, C. Wandel, B. Leake, A. J. Wood, D. M. Roden, and G. R. Wilkinson. The drug transporter P-glycoprotein limits oral absorption and brain entry of HIV-1 protease inhibitors. *J. Clin. Invest.* **101**:289–294 (1998).
9. G. Y. Kwei, R. F. Alvaro, Q. Chen, H. J. Jenkins, C. E. Hop, C. A. Keohane, V. T. Ly, J. R. Strauss, R. W. Wang, Z. Wang, T. R. Pippert, and D. R. Umbenhauer. Disposition of ivermectin and cyclosporin A in CF-1 mice deficient in mdr1a P-glycoprotein. *Drug Metab. Dispos.* **27**:581–587 (1999).

10. A. Sparreboom, J. van Asperen, U. Mayer, A. H. Schinkel, J. W. Smit, D. K. Meijer, P. Borst, W. J. Nooijen, J. H. Beijnen, and O. van Tellingen. Limited oral bioavailability and active epithelial excretion of paclitaxel (Taxol) caused by P-glycoprotein in the intestine. *Proc. Natl. Acad. Sci. USA* **94**:2031–2035 (1997).
11. W. L. Chiou, S. M. Chung, and T. C. Wu. Commentary: Potential role of P-glycoprotein in affecting hepatic metabolism of drugs. *Pharm. Res.* **17**:901–903 (2000).
12. K. Arimori and M. Nakano. Drug exsorption from blood into the gastrointestinal tract. *Pharm. Res.* **15**:371–376 (1998).
13. J. van Asperen, O. van Tellingen, and J. H. Beijnen. The role of mdr1a P-glycoprotein in the biliary and intestinal secretion of doxorubicin and vinblastine in mice. *Drug Metab. Dispos.* **28**:264–267 (2000).
14. U. Mayer, E. Wagenaar, J. H. Beijnen, J. W. Smit, D. K. Meijer, J. van Asperen, P. Borst, and A. H. Schinkel. Substantial excretion of digoxin via the intestinal mucosa and prevention of long-term digoxin accumulation in the brain by the mdr 1a P-glycoprotein. *Br. J. Pharmacol.* **119**:1038–1044 (1996).
15. B. Greiner, M. Eichelbaum, P. Fritz, H. P. Kreichgauer, O. von Richter, J. Zundler, and H. K. Kroemer. The role of intestinal P-glycoprotein in the interaction of digoxin and rifampin. *J. Clin. Invest.* **104**:147–153 (1999).
16. H. Diddens, V. Gekeler, M. Neumann, and D. Niethammer. Characterization of actinomycin-D-resistant CHO cell lines exhibiting a multidrug-resistance phenotype and amplified DNA sequences. *Int. J. Cancer* **40**:635–642 (1987).
17. J. S. Lee, K. Paull, M. Alvarez, C. Hose, A. Monks, M. Grever, A. T. Fojo, and S. E. Bates. Rhodamine efflux patterns predict P-glycoprotein substrates in the National Cancer Institute drug screen. *Mol. Pharmacol.* **46**:627–638 (1994).
18. R. Yumoto, T. Murakami, Y. Nakamoto, R. Hasegawa, J. Nagai, and M. Takano. Transport of rhodamine 123, a P-glycoprotein substrate, across rat intestine and Caco-2 cell monolayers in the presence of cytochrome P-450 3A-related compounds. *J. Pharmacol. Exp. Ther.* **289**:149–155 (1999).
19. M. Takano, R. Hasegawa, T. Fukuda, R. Yumoto, J. Nagai, and T. Murakami. Interaction with P-glycoprotein and transport of erythromycin, midazolam and ketoconazole in Caco-2 cells. *Eur. J. Pharmacol.* **358**:289–294 (1998).
20. M. D. Perloff, L. L. von Moltke, E. Stormer, R. I. Shader, and D. J. Greenblatt. Saint John's wort: an in vitro analysis of P-glycoprotein induction due to extended exposure. *Br. J. Pharmacol.* **134**:1601–1608 (2001).
21. J. M. Dintaman and J. A. Silverman. Inhibition of P-glycoprotein by D-alpha-tocopheryl polyethylene glycol 1000 succinate (TPGS). *Pharm. Res.* **16**:1550–1556 (1999).
22. S. Tansan, Y. Koc, H. Aydin, G. Urbano, and R. McCaffrey. Augmentation of vincristine cytotoxicity by megestrol acetate. *Cancer Chemother. Pharmacol.* **39**:333–340 (1997).
23. C. W. Cho, Y. Liu, X. Yan, T. Henthorn, and K. Y. Ng. Carrier-mediated uptake of rhodamine 123: implications on its use for MDR research. *Biochem. Biophys. Res. Commun.* **279**:124–130 (2000).
24. R. Masereeuw, M. M. Moons, and F. G. Russel. Rhodamine 123 accumulates extensively in the isolated perfused rat kidney and is secreted by the organic cation system. *Eur. J. Pharmacol.* **321**: 315–323 (1997).
25. I. C. van der Sandt, M. C. Blom-Roosemalen, A. G. de Boer, and D. D. Breimer. Specificity of doxorubicin versus rhodamine-123 in assessing P- glycoprotein functionality in the LLC-PK1, LLC-PK1:MDR1 and Caco-2 cell lines. *Eur. J. Pharm. Sci.* **11**:207–214 (2000).
26. P. Schmiedlin-Ren, K. E. Thummel, J. M. Fisher, M. F. Paine, K. S. Lown, and P. B. Watkins. Expression of enzymatically active CYP3A4 by Caco-2 cells grown on extracellular matrix-coated permeable supports in the presence of 1alpha,25-dihydroxy-vitamin D3. *Mol. Pharmacol.* **51**:741–754 (1997).
27. K. Lee and D. R. Thakker. Saturable transport of H2-antagonists ranitidine and famotidine across Caco-2 cell monolayers. *J. Pharm. Sci.* **88**:680–687 (1999).
28. L. S. Gan, P. H. Hsyu, J. F. Pritchard, and D. Thakker. Mechanism of intestinal absorption of ranitidine and ondansetron: transport across Caco-2 cell monolayers. *Pharm. Res.* **10**:1722–1725 (1993).
29. F. Hyafil, C. Vergely, P. Du Vignaud, and T. Grand-Perret. In vitro and in vivo reversal of multidrug resistance by GF120918, an acridonecarboxamide derivative. *Cancer Res.* **53**:4595–4602 (1993).
30. P. F. Augustijns, T. P. Bradshaw, L. S. Gan, R. W. Hendren, and D. R. Thakker. Evidence for a polarized efflux system in CACO-2 cells capable of modulating cyclosporin A transport. *Biochem. Biophys. Res. Commun.* **197**:360–365 (1993).
31. J. Hunter, M. A. Jepson, T. Tsuruo, N. L. Simmons, and B. H. Hirst. Functional expression of P-glycoprotein in apical membranes of human intestinal Caco-2 cells. Kinetics of vinblastine secretion and interaction with modulators. *J. Biol. Chem.* **268**: 14991–14997 (1993).
32. A. B. Shapiro and V. Ling. Positively cooperative sites for drug transport by P-glycoprotein with distinct drug specificities. *Eur. J. Biochem.* **250**:130–137 (1997).
33. M. A. Hurni, A. B. Noach, M. C. Blom-Roosemalen, A. G. de Boer, J. F. Nagelkerke, and D. D. Breimer. Permeability enhancement in Caco-2 cell monolayers by sodium salicylate and sodium taurodihydrofusidate: assessment of effect-reversibility and imaging of transepithelial transport routes by confocal laser scanning microscopy. *J. Pharmacol. Exp. Ther.* **267**:942–950 (1993).
34. T. J. Lampidis, C. Castello, A. del Giglio, B. C. Pressman, P. Viallet, K. W. Trevorrow, G. K. Valet, H. Tapiero, and N. Savaraj. Relevance of the chemical charge of rhodamine dyes to multiple drug resistance. *Biochem. Pharmacol.* **38**:4267–4271 (1989).
35. F. Ingels, S. Deferme, E. Destexhe, M. Oth, G. Van den Mooter, and P. Augustijns. Simulated intestinal fluid as transport medium in the Caco-2 cell culture model. *Int. J. Pharm.* **232**:183–192 (2002).
36. L. P. Rivory, K. M. Avent, and S. M. Pond. Effects of lipophilicity and protein binding on the hepatocellular uptake and hepatic disposition of two anthracyclines, doxorubicin and iododoxorubicin. *Cancer Chemother. Pharmacol.* **38**:439–445 (1996).
37. G. A. Altenberg, C. G. Vanoye, J. K. Horton, and L. Reuss. Unidirectional fluxes of rhodamine 123 in multidrug-resistant cells: evidence against direct drug extrusion from the plasma membrane. *Proc. Natl. Acad. Sci. USA* **91**:4654–4657 (1994).
38. G. van Meer and K. Simons. The function of tight junctions in maintaining differences in lipid composition between the apical and the basolateral cell surface domains of MDCK cells. *EMBO J.* **5**:1455–1464 (1986).
39. A. Collett, N. B. Higgs, E. Sims, M. Rowland, and G. Warhurst. Modulation of the permeability of H2 receptor antagonists cimetidine and ranitidine by P-glycoprotein in rat intestine and the human colonic cell line Caco-2. *J. Pharmacol. Exp. Ther.* **288**: 171–178 (1999).
40. M. D. Troutman and D. R. Thakker. Novel experimental parameters to quantify the modulation of absorptive and secretory transport of compounds by P-glycoprotein in cell culture. Models of intestinal epithelium. *Pharm. Res.* **20**:1210–1224 (2003).